



This is a repository copy of *Disturbance attenuation in the Euler-Bernoulli beam using piezoelectric actuators*.

White Rose Research Online URL for this paper:

<https://eprints.whiterose.ac.uk/207311/>

Version: Submitted Version

Preprint:

Selivanov, A. orcid.org/0000-0001-5075-7229 and Fridman, E. (Submitted: 2023)

Disturbance attenuation in the Euler-Bernoulli beam using piezoelectric actuators. [Preprint - arXiv] (Submitted)

<https://doi.org/10.48550/arXiv.2308.05551>

© 2023 The Author(s). For reuse permissions, please contact the Author(s).

Reuse

Items deposited in White Rose Research Online are protected by copyright, with all rights reserved unless indicated otherwise. They may be downloaded and/or printed for private study, or other acts as permitted by national copyright laws. The publisher or other rights holders may allow further reproduction and re-use of the full text version. This is indicated by the licence information on the White Rose Research Online record for the item.

Takedown

If you consider content in White Rose Research Online to be in breach of UK law, please notify us by emailing eprints@whiterose.ac.uk including the URL of the record and the reason for the withdrawal request.



eprints@whiterose.ac.uk
<https://eprints.whiterose.ac.uk/>

Disturbance attenuation in the Euler-Bernoulli beam using piezoelectric actuators

Anton Selivanov^a, Emilia Fridman^b

^a*Department of Automatic Control and Systems Engineering, The University of Sheffield, UK*

^b*School of Electrical Engineering, Tel Aviv University, Israel*

Abstract

We consider a simply-supported Euler–Bernoulli beam with viscous and Kelvin–Voigt damping. Our objective is to attenuate the effect of an unknown distributed disturbance using one piezoelectric actuator. We show how to design a suitable H_∞ state-feedback controller based on a finite number of dominating modes. If the remaining (infinitely many) modes are ignored, the calculated L^2 gain is wrong. This happens because of the spillover phenomenon that occurs when the effect of the control on truncated modes is not accounted for in the feedback design. We propose a simple modification of the H_∞ cost that prevents spillover. The key idea is to treat the control as a disturbance in the truncated modes and find the corresponding L^2 gains using the bounded real lemma. These L^2 gains are added to the control weight in the H_∞ cost for the dominating modes, which prevents spillover. A numerical simulation of an aluminum beam with realistic parameters demonstrates the effectiveness of the proposed method.

Key words: Distributed parameter systems; Euler–Bernoulli beam; H_∞ control; modal decomposition.

1 Introduction

One of the main challenges in extending the H_∞ theory to infinite-dimensional systems is to obtain *finite-dimensional* controllers, which are easy to implement. A direct extension of the frequency domain approach leads to infinite-dimensional controllers [1,2], which can be approximated with finite-dimensional ones by sacrificing the optimality. Alternatively, one can perform modal decomposition [3,4] and design a controller for a finite number of dominating modes [5,6,7,8]. However, such a controller may have a deteriorating effect on the neglected modes [9,10,11], which is called the “spillover” phenomenon. Spillover can be reduced (but not avoided) by introducing a residual filter accounting for a finite number of additional modes [12,13,14].

Performance analysis requires a more accurate treatment of the residue. In particular, the input-to-state stability of parabolic PDEs with respect to boundary disturbances was established in [15] by analyzing the residue. Later, modal

decomposition was combined with Lyapunov functionals to design finite-dimensional *state-feedback* [16] and finite-dimensional *output-feedback* [17,18] control for parabolic PDEs. These results were subsequently extended to input/output delays [19,18], semilinear systems [20], and the Kuramoto–Sivashinsky equation [21]. In particular, [21] designed a finite-dimensional H_∞ output feedback and provided linear matrix inequalities (LMIs) to find the corresponding L^2 gain. In [22], we extended this LMI-based approach to the Euler–Bernoulli beam with piezoelectric actuators. However, the derived LMIs are conservative and require considering many modes in the design.

Disturbance attenuation in flexible structures using piezoelectric actuators is of great importance for aerospace, civil, and mechanical engineering [23,24]. The frequency domain approach to H_∞ control of beams was developed in [25,26]. The controllability problem for the beam with piezoelectric actuators was studied in [27,28]. Boundary disturbances and actuators were considered in [29,30]. An experimental study of the disturbance attenuation with piezoelectric sensors and actuators (without a spillover analysis) was reported in [31,32].

This paper proposes a method of designing a finite-dimensional H_∞ controller for the Euler–Bernoulli beam that completely avoids spillover. Our main idea is to design a controller for a finite number of dominating modes

* Emilia Fridman is supported by ISF 673/19. This paper was submitted for publication in *Automatica*. The preliminary version of the paper was accepted for presentation at IEEE Conference on Decision and Control 2023.

Email addresses: a.selivanov@sheffield.ac.uk (Anton Selivanov), emilia@tauex.tau.ac.il (Emilia Fridman).

and treat it as a disturbance in the remaining modes. We explicitly solve the algebraic Riccati equation for each neglected mode to find the control-to-state L^2 gains. These gains are added to the control weight in the cost used to design an H_∞ controller for the dominating modes. We prove that this modification prevents spillover. Using an example of an aluminum beam with realistic parameters, we demonstrate how our approach avoids the spillover phenomenon. Compared to [22], the results of this paper are less conservative, more intuitive, and avoid spillover when arbitrarily few modes are used in the control design. Moreover, we prove that the L^2 gain can only decrease when more modes are considered. These improvements were achieved using the cost decomposition idea, presented in Section 3.3, and by replacing the Lyapunov equations for the residue with suitable algebraic Riccati equations (see (20)).

Notations: $|\cdot|$ is the Euclidean norm, $\|\cdot\|$ is the L^2 norm, $\langle \cdot, \cdot \rangle$ is the scalar product in L^2 , $H^p(0, \pi)$ with $p \in \mathbb{N}$ are the Sobolev spaces, $H^{-p}(0, \pi)$ are their dual spaces, $\text{diag}\{\omega_1, \dots, \omega_N\}$ is the diagonal matrix with diagonal elements ω_n , $n = 1, \dots, N$. For a matrix P , the notation $P < 0$ implies that P is square, symmetric, and negative-definite. Partial derivatives are denoted by indices, e.g., $z_t = \partial z / \partial t$.

1.1 Preliminaries: H_∞ control of finite-dimensional systems

Consider the LTI system

$$\begin{aligned} \dot{x}(t) &= Ax(t) + Bu(t) + Ev(t), & x(0) &= 0, \\ y(t) &= Cx(t) + Du(t) \end{aligned} \quad (1)$$

with state $x \in \mathbb{R}^n$, control input $u \in \mathbb{R}^m$, disturbance $v \in \mathbb{R}^k$, controlled output $y \in \mathbb{R}^l$, and constant matrices A , B , C , D , and E . For a given L^2 gain $\gamma > 0$, the H_∞ control problem is to find $u \in L^2([0, \infty), \mathbb{R}^m)$ guaranteeing

$$\int_0^\infty [|y(t)|^2 - \gamma^2 |v(t)|^2] dt \leq 0, \quad \forall v \in L^2([0, \infty), \mathbb{R}^k). \quad (2)$$

The proofs of the following results are given, e.g., in [33].

Proposition 1 Consider (1) such that $D^\top C = 0$ and $R = D^\top D > 0$. Given $\gamma > 0$, let $0 < P \in \mathbb{R}^{n \times n}$ satisfy

$$PA + A^\top P + P(\gamma^{-2}EE^\top - BR^{-1}B^\top)P + C^\top C = 0. \quad (3)$$

Then $u(t) = -R^{-1}B^\top Px(t)$ guarantees (2).

Remark 1 (Solution existence) If (A, B) is stabilizable, (A, C) is detectable, and γ is large enough, then (3) has a solution. For this solution, the closed-loop matrix $A - BR^{-1}B^\top P$ is stable.

Corollary 1 (Bounded Real Lemma) Consider (1) with $B = 0$ and $D = 0$ (i.e., without control). Given $\gamma > 0$, let $0 < P \in \mathbb{R}^{n \times n}$ satisfy

$$PA + A^\top P + \gamma^{-2}PEE^\top P + C^\top C = 0. \quad (4)$$

Then (2) holds without control.

Remark 2 (Initial state and worst disturbance) If $x(0) \neq 0$ in (1), then the (closed-loop) system must be internally stable (i.e., for $v \equiv 0$), and the left-hand side of (2) must include an additional term, $x^\top(0)Px(0)$. In this case, the disturbance maximizing (2) for the optimal control $u(t) = -R^{-1}B^\top Px(t)$ is

$$v(t) = \gamma^{-2}E^\top Px(t),$$

where $P > 0$ is a solution of (3). Without control, the worst disturbance is the same, but $P > 0$ must solve (4).

2 Model description

2.1 Euler–Bernoulli beam with control and disturbance

We consider the Euler–Bernoulli beam described by

$$\begin{aligned} \mu \tilde{z}_{tt}(x, t) + EI \tilde{z}_{xxxx}(x, t) + c_v \tilde{z}_t(x, t) + c_k I \tilde{z}_{xxxxt}(x, t) = \\ c_a [\delta'(x - \tilde{x}_L) - \delta'(x - \tilde{x}_R)] \tilde{u}(t) + \tilde{w}(x, t), \\ \tilde{z}(0, t) = \tilde{z}_{xx}(0, t) = \tilde{z}(L, t) = \tilde{z}_{xx}(L, t) = 0, \end{aligned} \quad (5)$$

where $\tilde{z}: [0, L] \times [0, \infty) \rightarrow \mathbb{R}$ is the transverse deflection of a beam of length L , linear density μ , Young’s modulus of elasticity E , and moment of inertia I . The model accounts for the viscous damping $c_v \tilde{z}_t$ and structural (Kelvin–Voigt) damping $c_k I \tilde{z}_{xxxxt}$ [34,35]. A piezoelectric actuator produces bending moments at $\tilde{x}_L, \tilde{x}_R \in (0, L)$ proportional to the applied voltage $\tilde{u}: [0, \infty) \rightarrow \mathbb{R}$. Following [23,27], we model it using the derivative of the Dirac delta function, $\delta'(\cdot - \tilde{x}) \in H^{-2}(0, L)$, defined as

$$\delta'(\cdot - \tilde{x})f = \int_0^L \delta'(x - \tilde{x})f(x) dx = -f'(\tilde{x}) \quad (6)$$

for any $\tilde{x} \in (0, L)$ and $f \in H^2(0, L)$. The external disturbance is represented by $\tilde{w}: (0, L) \times [0, \infty) \rightarrow \mathbb{R}$. All the parameters are constant in time and space. The boundary conditions correspond to the hinged ends.

Remark 3 (Damping model) The Kelvin–Voigt damping is motivated by the experimental observation that damping rates in beams increase with frequency [34]. This is also captured by the “square root” model given by $-c_r \tilde{z}_{xxt}$ [36]. Our analysis can be extended to the “square root” model straightforwardly.

By scaling the space and time as follows

$$z(x, t) = \tilde{z}(a_1 x, a_2 t), \quad a_1 = \frac{L}{\pi}, \quad a_2 = a_1^2 \sqrt{\frac{\mu}{EI}}, \quad (7)$$

we rewrite (5) as

$$\begin{aligned} z_{tt} + z_{xxxx} + c_1 z_t + c_2 z_{xxxxt} = [\delta'_L - \delta'_R] u + w, \\ z(0, 0) = z_{xx}(0, 0) = z(\pi, 0) = z_{xx}(\pi, 0) = 0, \end{aligned} \quad (8)$$

where $x \in [0, \pi]$, $t \geq 0$,

$$\begin{aligned} c_1 &= \frac{c_v a_2}{\mu}, & c_2 &= \frac{c_k I a_2}{\mu a_1^4}, & x_L &= \frac{\tilde{x}_L}{a_1}, & x_R &= \frac{\tilde{x}_R}{a_1}, \\ \delta'_L &= \delta'(x - x_L), & \delta'_R &= \delta'(x - x_R), \\ u(t) &= \frac{c_a a_2^2}{\mu a_1^2} \tilde{u}(a_2 t), & w(x, t) &= \frac{a_2^2}{\mu} \tilde{w}(a_1 x, a_2 t). \end{aligned}$$

Note that (6) implies $\delta'(a_1 x - \tilde{x}) = \delta'(x - \tilde{x}/a_1)/a_1^2$. To simplify further derivations, we assume that

$$c_1 + c_2 \leq \sqrt{2}. \quad (9)$$

That is, the dynamics are dominated by the elasticity rather than damping. The extension to $c_1 + c_2 > \sqrt{2}$ is straightforward but cumbersome.

2.2 Well-posedness

Define the Hilbert spaces of the H^2 and H^4 functions that are consistent with the boundary conditions:

$$\begin{aligned} H_{BC}^2(0, \pi) &= \{f \in H^2(0, \pi) \mid f(0) = 0 = f(\pi)\}, \\ H_{BC}^4(0, \pi) &= \left\{ f \in H^4(0, \pi) \mid \begin{array}{l} f(0) = f''(0) = 0 \\ f(\pi) = f''(\pi) = 0 \end{array} \right\}. \end{aligned}$$

The energy space of (8) is

$$X = H_{BC}^2(0, \pi) \times L^2(0, \pi)$$

with the scalar product

$$\langle (f_1, g_1), (f_2, g_2) \rangle_X = \langle f_1'', f_2'' \rangle_{L^2} + \langle g_1, g_2 \rangle_{L^2}.$$

Consider

$$\mathcal{A}_0 f = -f'', \quad D(\mathcal{A}_0) = H_{BC}^2(0, \pi) \subset L^2(0, \pi). \quad (10)$$

In the operator form, (8) is written as

$$\dot{\tilde{z}} = \mathcal{A} \tilde{z} + f, \quad (11)$$

where

$$\begin{aligned} \tilde{z}(t) &= \begin{bmatrix} z(\cdot, t) \\ z_t(\cdot, t) \end{bmatrix}, & \mathcal{A} &= \begin{bmatrix} 0 & I \\ -\mathcal{A}_0^2 & -(c_1 I + c_2 \mathcal{A}_0^2) \end{bmatrix}, \\ f(t) &= \begin{bmatrix} 0 \\ [\delta'_L - \delta'_R]u(t) + w(\cdot, t) \end{bmatrix}. \end{aligned}$$

Since $D(\mathcal{A}_0^2) = H_{BC}^4(0, \pi)$, we have

$$D(\mathcal{A}) = X_1 = H_{BC}^4(0, \pi) \times H_{BC}^4(0, \pi) \subset X.$$

The adjoint of \mathcal{A} with respect to the scalar product in X is

$$\mathcal{A}^* = \begin{bmatrix} 0 & -I \\ \mathcal{A}_0^2 & -(c_1 I + c_2 \mathcal{A}_0^2) \end{bmatrix}, \quad D(\mathcal{A}^*) = X_1 \subset X.$$

Since \mathcal{A} and \mathcal{A}^* are dissipative, \mathcal{A} generates a C_0 -semigroup of contractions on X [37, Corollary 4.4].

The set $D(\mathcal{A}^*)$ with the norm $\|z\|_1^d = \|(\beta I - \mathcal{A}^*)z\|$, where β is any regular point of \mathcal{A} , is a Hilbert space. Its dual is $X_{-1} = H^{-4}(0, \pi) \times H^{-4}(0, \pi)$.

We assume that

$$w \in H_{loc}^1((0, \infty), X_{-1}) \cap L^2((0, \infty), L^2(0, \pi)). \quad (12)$$

The control input that we design later satisfies $u \in H_{loc}^1((0, \infty), \mathbb{R})$. Therefore,

$$[\delta'_L - \delta'_R]u \in H_{loc}^1((0, \infty), H^{-2}(0, \pi)).$$

This implies $f \in H_{loc}^1((0, \infty), X_{-1})$. By [38, Theorem 4.1.6], for $z(\cdot, 0) \in H_{BC}^2(0, \pi)$ and $z_t(\cdot, 0) \in L^2(0, \pi)$, there exists a unique solution of (11) in X_{-1} that satisfies

$$\tilde{z} \in C([0, \infty); X) \cap C^1([0, \infty); X_{-1}).$$

That is

$$\begin{aligned} z &\in C([0, \infty); H^2(0, \pi)) \cap C^1([0, \infty); H^{-4}(0, \pi)), \\ z_t &\in C([0, \infty); L^2(0, \pi)) \cap C^1([0, \infty); H^{-4}(0, \pi)). \end{aligned}$$

Remark 4 We need $w \in H_{loc}^1((0, \infty), X_{-1})$ only to guarantee that $z(t, \cdot) \in H^2$ and $z_t(t, \cdot) \in L^2$ for $t \geq 0$, which is required for the modal decomposition in Section 3.1.

3 Full-information H_∞ control of the beam

Given non-negative scalars ρ_x , ρ_u , and γ , our objective is to find a state-feedback control law guaranteeing that the trajectories of (8) with $z(\cdot, 0) \equiv 0 \equiv z_t(\cdot, 0)$ satisfy (cf. (2))

$$\begin{aligned} J = \int_0^\infty & \left[\|z(\cdot, t)\|^2 + \rho_x \|z_{xx}(\cdot, t)\|^2 \right. \\ & \left. + \rho_u u^2(t) - \gamma^2 \|w(\cdot, t)\|^2 \right] dt \leq 0 \quad (13) \end{aligned}$$

for all w satisfying (12). Such control guarantees that the L^2 gain is not greater than γ .

Remark 5 (Performance index) Since the potential energy of (5) due to bending is $\frac{EI}{2} \|\tilde{z}_{xx}(\cdot, t)\|^2$ [39, p. 317], we include $\|z_{xx}(\cdot, t)\|^2$ in (13). Note that Wirtinger's inequality [40] implies $\|z(\cdot, t)\| \leq 2\|z_{xx}(\cdot, t)\|$. Therefore, $\|z(\cdot, t)\|^2$ could be omitted in (13), but we kept it to render (13) more intuitive. The kinetic energy of (5) is $\frac{\rho}{2} \|\tilde{z}_t(\cdot, t)\|^2$, and it is natural to include $\|z_t(\cdot, t)\|^2$ in (13). To simplify the exposition, we do not present this extension, which requires one to consider multiple cases depending on the values of c_1 , c_2 , ρ_x , and ρ_u .

3.1 Modal decomposition

The modes and natural frequencies of (8) are

$$\varphi_n(x) = \sqrt{2/\pi} \sin nx, \quad \omega_n = n^2, \quad n \in \mathbb{N}.$$

These are the eigenfunctions and eigenvalues of \mathcal{A}_0 defined in (10), which form a complete orthonormal system in $L^2(0, \pi)$. Therefore,

$$z(\cdot, t) \stackrel{L^2}{=} \sum_{n=1}^{\infty} z_n(t) \varphi_n, \quad z_n(t) = \langle z(\cdot, t), \varphi_n \rangle.$$

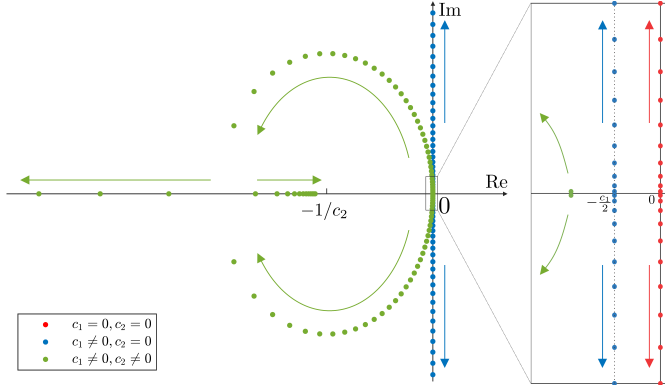


Fig. 1. The eigenvalues of A_n given in (15) for $n = 1, \dots, 50$. Red dots — no damping ($c_1 = 0 = c_2$); blue dots — viscous damping ($c_1 = 1.4 \times 10^{-3}$, $c_2 = 0$); green dots — viscous and Kelvin–Voigt damping ($c_1 = 1.4 \times 10^{-3}$, $c_2 = 1.3 \times 10^{-3}$).

Substituting this into (8), in view of

$$\langle \delta'_L, \varphi_n \rangle \stackrel{(6)}{=} -\varphi'_n(x_L) \quad \text{and} \quad \langle \delta'_R, \varphi_n \rangle \stackrel{(6)}{=} -\varphi'_n(x_R),$$

we obtain the ODEs for the Fourier coefficients

$$\ddot{z}_n(t) + 2\zeta_n\omega_n\dot{z}_n(t) + \omega_n^2 z_n(t) = b_n u(t) + w_n(t), \quad n \in \mathbb{N},$$

where

$$\zeta_n = (c_1\omega_n^{-1} + c_2\omega_n)/2,$$

$$b_n = n\sqrt{2/\pi}(\cos nx_R - \cos nx_L),$$

$$w_n(t) = \langle w(\cdot, t), \varphi_n \rangle.$$

The ODEs can be written as

$$\dot{\bar{z}}_n(t) = A_n \bar{z}_n(t) + B_n u(t) + E_n w_n(t), \quad n \in \mathbb{N}, \quad (14)$$

where

$$\bar{z}_n = \begin{bmatrix} z_n \\ \dot{z}_n \end{bmatrix}, A_n = \begin{bmatrix} 0 & 1 \\ -\omega_n^2 & -2\zeta_n\omega_n \end{bmatrix}, B_n = \begin{bmatrix} 0 \\ b_n \end{bmatrix}, E_n = \begin{bmatrix} 0 \\ 1 \end{bmatrix}.$$

The eigenvalues of A_n are

$$\lambda_n^\mp = -\omega_n(\zeta_n \pm \sqrt{\zeta_n^2 - 1}). \quad (15)$$

Without damping ($\zeta_n = 0$), infinitely many imaginary roots $\lambda_n^\pm = \pm i\omega_n$ (see Fig. 1) give rise to free vibrations in (8) in the absence of control and disturbance. Our approach does not work in this case since it is not enough to deal only with a finite number of modes. Viscous damping ($c_1 \neq 0$) ensures that $\text{Re } \lambda_n^\pm = -c_1/2$. Kelvin–Voigt damping ($c_2 \neq 0$) improves the stability further guaranteeing

$$\text{Re } \lambda_n^- \rightarrow -\infty \quad \text{and} \quad \text{Re } \lambda_n^+ \rightarrow -1/c_2.$$

We develop our approach for the case when $c_1 \neq 0 \neq c_2$.

3.2 The spillover phenomenon

It is common in engineering practice to design controllers based on a few dominating modes while ignoring the residue. This subsection demonstrates that such an approach may suffer from the spillover phenomenon.

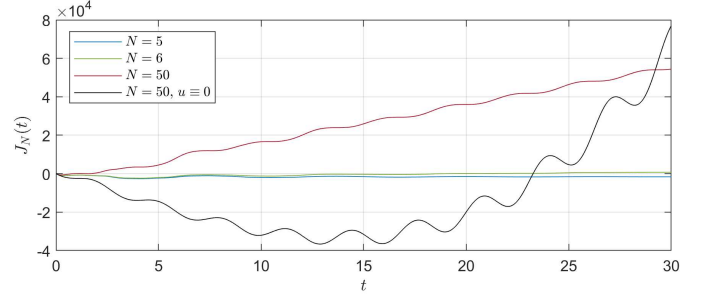


Fig. 2. The value of $J_N(t)$, defined in (16), for $N = 5$ (blue), $N = 6$ (green), and $N = 50$ (red). The black line is $J_N(t)$ for $N = 50$ and $u \equiv 0$. A controller designed for the first 5 modes cannot guarantee (13) for the original system because of the spillover phenomenon.

Consider the Euler–Bernoulli beam (8) with

$$c_1 = 1.4 \times 10^{-3}, \quad c_2 = 1.3 \times 10^{-3}, \quad x_L = 0.91, \quad x_R = 0.97.$$

The choice of the parameters is explained in Section 4. Let us try to design a controller guaranteeing (13) with $\rho_x = 0.1$ and $\rho_u = 10^{-3}$ by considering only 5 modes in the modal decomposition (14). Using Proposition 1 (see Section 3.5 for details), we find $\gamma \approx 6.97$ and the corresponding controller gain $-R^{-1}B^\top P \in \mathbb{R}^{1 \times 10}$.

Figure 2 shows the values of

$$J_N(t) = \int_0^t \left[\sum_{n=1}^N [(1 + \rho_x \omega_n^2) z_n^2(t) - \gamma^2 w_n^2(t)] + \rho_u u^2(t) \right] dt \quad (16)$$

for different numbers of modes, N . Proposition 1 guarantees $J_5(t) \leq 0$ (blue line). However, if we include one more mode without adjusting γ and the controller, $J_6(t)$ becomes positive for $t > 20$ (green line). The red line shows $J_{50}(t) \approx J_\infty(t)$. Clearly, the controller designed using only 5 modes cannot guarantee (13) for the original system.

Spillover occurs because the effect of the controller on the truncated modes is ignored. In the remainder of the paper, we provide a simple remedy to avoid spillover. Namely, we show how to modify ρ_u in (16) so that a controller guaranteeing $J_N(t) \leq 0$ for a given N will guarantee (13) with the original ρ_u .

3.3 Cost decomposition

We represent (14) as

$$\dot{z}^N = Az^N + Bu + Ew^N, \quad (17a)$$

$$\dot{\bar{z}}_n = A_n \bar{z}_n + B_n u + E_n w_n, \quad n > N, \quad (17b)$$

where $N \in \mathbb{N}$,

$$z^N = \begin{bmatrix} z_1 \\ \vdots \\ z_N \\ \dot{z}_1 \\ \vdots \\ z_N \end{bmatrix}, \quad w^N = \begin{bmatrix} w_1 \\ \vdots \\ w_N \end{bmatrix}, \quad B = \begin{bmatrix} 0 \\ \vdots \\ \dot{0} \\ b_1 \\ \vdots \\ b_N \end{bmatrix}, \quad E = \begin{bmatrix} 0_N \\ I_N \end{bmatrix},$$

$$A = \begin{bmatrix} 0_N & I_N \\ -\Omega_N^2 & -(c_1 I_N + c_2 \Omega_N^2) \end{bmatrix}, \quad \Omega_N = \text{diag}\{\omega_1, \dots, \omega_N\},$$
(18)

and the remaining notations are from (14). We will design an H_∞ controller for (17a) with the cost, J_0 , that accounts for its effect on (17b). To find this cost, we decompose the original cost J from (13). Namely, since $z(\cdot, t) \in H^2(0, \pi)$ (see Section 2.2), Parseval's identity gives

$$\|z(\cdot, t)\|^2 = \sum_{n=1}^{\infty} z_n^2(t), \quad \|z_{xx}(\cdot, t)\|^2 = \sum_{n=1}^{\infty} \omega_n^2 z_n^2(t).$$

Our key idea is to represent J from (13) as

$$J = J_0 + \sum_{n=N+1}^{\infty} J_n, \quad (19)$$

where

$$J_0 = \int_0^\infty \left[\sum_{n=1}^N (1 + \rho_x \omega_n^2) z_n^2 + (\rho_u + \sum_{n=N+1}^{\infty} \rho_n) u^2 - \gamma^2 \sum_{n=1}^N w_n^2 \right],$$

$$J_n = \int_0^\infty [(1 + \rho_x \omega_n^2) z_n^2 - \rho_n u^2 - \gamma^2 w_n^2].$$

The control, $u(t)$, is treated as a disturbance in (17b). Using the bounded real lemma (Corollary 1), we will find the minimum ρ_n such that $J_n \leq 0$ for the zero initial conditions and any $w_n \in L^2([0, \infty), \mathbb{R})$. Then, we will show that $\sum_{n=N+1}^{\infty} \rho_n < \infty$ and construct a controller for (17a) guaranteeing $J_0 \leq 0$.

3.4 Bounded real lemma for the residue

For a given $n > N$, (17b) can be represented as (1) with $x = \bar{z}_n$, $A = A_n$, $B = 0_{2 \times 1}$,

$$v = \begin{bmatrix} \sqrt{\rho_n} u / \gamma \\ \frac{\gamma}{\sqrt{\rho_n}} B_n E_n \end{bmatrix}.$$

Note that the control input, u , is considered as a part of the disturbance, v , since the H_∞ control will be designed based on (17a). The cost in (2) coincides with J_n for

$$C = \begin{bmatrix} \sqrt{1 + \rho_x \omega_n^2} & 0 \end{bmatrix} \quad \text{and} \quad D = 0.$$

Then the algebraic Riccati equation (4) takes the form

$$P_n A_n + A_n^\top P_n + \gamma^{-2} P_n \begin{bmatrix} 0 & 0 \\ 1 + \gamma^2 b_n^2 / \rho_n & 0 \end{bmatrix} P_n + \begin{bmatrix} 1 + \rho_x \omega_n^2 & 0 \\ 0 & 0 \end{bmatrix} = 0. \quad (20)$$

In Appendix A, we show that the smallest ρ_n guaranteeing the feasibility of (20) is

$$\rho_n = \begin{cases} \frac{b_n^2 (1 + \rho_x \omega_n^2)}{4\omega_n^4 \zeta_n^2 (1 - \zeta_n^2) - (1 + \rho_x \omega_n^2) \gamma^{-2}} & \text{if } 2\zeta_n^2 \leq 1, \\ \frac{b_n^2 (1 + \rho_x \omega_n^2)}{\omega_n^4 - (1 + \rho_x \omega_n^2) \gamma^{-2}} & \text{if } 2\zeta_n^2 > 1. \end{cases}$$

The value of ρ_n is the L^2 gain from u to \bar{z}_n . Corollary 1 guarantees $J_n \leq 0$ for these ρ_n . This can be used to obtain the L^2 gain of (8) without control.

Proposition 2 (L^2 gain without control) *The L^2 gain of the control-free (8) subject to (9) is not greater than*

$$\gamma_0 = \frac{2\sqrt{1 + \rho_x}}{(c_1 + c_2)\sqrt{4 - (c_1 + c_2)^2}}.$$

Proof. Repeating the arguments of Appendix A with $\alpha_n = \gamma^{-2}$, we obtain that (20) is feasible for any $n \in \mathbb{N}$ if

$$\gamma^2 \geq \frac{1 + \rho_x \omega_n^2}{4\omega_n^4 \zeta_n^2 (1 - \zeta_n^2)} \quad \text{when } 2\zeta_n^2 \leq 1, \quad (21a)$$

$$\gamma^2 \geq \frac{1 + \rho_x \omega_n^2}{\omega_n^4} \quad \text{when } 2\zeta_n^2 > 1. \quad (21b)$$

The right-hand sides of (21) are decreasing in n . Moreover,

$$\omega_n^4 - 4\omega_n^4 \zeta_n^2 (1 - \zeta_n^2) = \omega_n^4 (1 - 2\zeta_n^2)^2 \geq 0$$

implies that the bound in (21a) is not smaller than in (21b). Since (9) guarantees $2\zeta_1^2 \leq 1$, the lower bound on γ is obtained from (21a) with $n = 1$, i.e., with $\omega_1 = 1$ and $\zeta_1 = (c_1 + c_2)/2$. The feasibility of (20) implies $J_n \leq 0$. Taking $N = 0$ and $J_0 = 0$ in (19), we obtain $J \leq 0$. \square

In Appendix B, we show that

$$\sum_{n=N+1}^{\infty} \rho_n \leq \rho_\infty = \sum_{n=N+1}^M \rho_n + C_M \left[|x_R - x_L| - \sum_{n=1}^M \frac{b_n^2}{\omega_n^2} \right], \quad (22)$$

where

$$C_M = \frac{\omega_{M+1}^2 (1 + \rho_x \omega_{M+1}^2)}{\omega_{M+1}^4 - (1 + \rho_x \omega_{M+1}^2) \gamma^{-2}},$$

$$M = \max \left\{ N, \left\lfloor \sqrt{\frac{1 + \sqrt{1 - 2c_1 c_2}}{\sqrt{2} c_2}} \right\rfloor \right\}.$$

Here, $\lfloor \cdot \rfloor$ stands for the integer part. Note that (9) implies $2c_1 c_2 \leq 1$.

As explained in Appendix B, $\sum_{n=1}^{\infty} b_n^2 / \omega_n^2 = |x_R - x_L|$. Therefore, $\rho_\infty \rightarrow 0$ monotonically as $N \rightarrow \infty$. That is, by considering more modes in the control design, we reduce the L^2 gain of the residue associated with the spillover.

Remark 6 (Control as structured disturbance) *To simplify the residue analysis, we treated u as an arbitrary disturbance when looking for ρ_n . Since we are designing the control, we can restrict the class of admissible u and, possibly, decrease ρ_n . This improvement is a direction for future research, which will rely on extending the H_∞ control to structured disturbances.*

3.5 H_∞ controller design without spillover

The system (17a) is in the form of (1) with $x = z^N$, $v = w^N$, and A , B , and E defined in (18). Taking

$$C = \begin{bmatrix} \sqrt{I_N + \rho_x \Omega_N^2} & 0_{N \times N} \\ 0_{1 \times N} & 0_{1 \times N} \end{bmatrix} \quad \text{and} \quad D = \begin{bmatrix} 0_{N \times 1} \\ \sqrt{\rho_u + \rho_\infty} \end{bmatrix}, \quad (23)$$

we obtain that $D^\top C = 0$, $R = D^\top D = \rho_u + \rho_\infty > 0$, and the left-hand side of (2) coincides with J_0 from (19). By Proposition 1, if $0 < P \in \mathbb{R}^{2N \times 2N}$ satisfies (3), then

$$u(t) = -(\rho_u + \rho_\infty)^{-1} B^\top P z^N(t) \quad (24)$$

guarantees $J_0 \leq 0$. Since ρ_n were chosen so that $J_n \leq 0$, we obtain that $J \leq 0$. We have proved the following theorem.

Theorem 1 *Consider the Euler–Bernoulli beam (8) subject to (9) and its modal decomposition (17) with some $N \in \mathbb{N}$. Given non-negative ρ_x , ρ_u , and γ , let ρ_∞ be given by (22). If $0 < P \in \mathbb{R}^{2N \times 2N}$ satisfies the algebraic Riccati equation (3) with A , B , C , D , and E given in (18) and (23), then the state feedback (24) guarantees that the L^2 gain of (8) is not greater than γ , that is, (13) holds for $z(\cdot, 0) \equiv 0 \equiv z_t(\cdot, 0)$ and any w satisfying (12).*

An alternative proof is to consider

$$V = (z^N)^\top P z^N + \sum_{n=N+1}^{\infty} \bar{z}_n^\top P_n \bar{z}_n$$

with P_n defined in Appendix A. Note that the series converges since

$$P_n \sim \rho_x \begin{bmatrix} \omega_n^2 c_2 & 1 \\ 1 & 2c_2 \end{bmatrix} \quad \text{as } n \rightarrow \infty \quad (25)$$

(we chose “+” for the right bottom element), while $z(\cdot, t) \in H^2(0, \pi)$ and $z_t(\cdot, t) \in L^2(0, \pi)$ (see Section 2.2). Using (3) and (20), one can show that

$$\dot{V}(t) + J(t) \leq 0, \quad (26)$$

where $J(t)$ is J defined in (13) with ∞ replaced by t . Integrating the above from 0 to t , we obtain

$$V(t) - V(0) + J(t) - J(0) \leq 0.$$

Given that $V(0) = 0$ for the zero initial conditions, and $J(0) = 0$, we have $J(t) \leq -V(t) \leq 0$, which implies (13).

Remark 7 (Internal stability) *The designed feedback (24) renders (8) internally stable in the norm*

$$\|z(\cdot, t)\|_X^2 = \|z_{xx}(\cdot, t)\|^2 + \|z_t(\cdot, t)\|^2.$$

Indeed, (25) implies the existence of positive ε_1 and ε_2 such that $\varepsilon_1 \|z(\cdot, t)\|_X^2 \leq V \leq \varepsilon_2 \|z(\cdot, t)\|_X^2$, and (26) implies $\dot{V} \leq 0$ for $w(\cdot, t) \equiv 0$.

Remark 8 (Solution existence) *Since A , defined in (18), is Hurwitz, (A, B) is stabilizable. It is easy to check that (A, C) is observable, hence detectable. As mentioned in Remark 1, this guarantees that (3) has a solution for a large enough γ . That is, the conditions of Theorem 1 hold for any $N \in \mathbb{N}$ and large enough γ .*

Remark 9 (Number of modes and the L^2 gain)

When N grows, γ can only decrease. Indeed, we know that $J_{N+1}(t) \leq 0$ and (24) guarantees $J_0(t) \leq 0$ with $J_{N+1}(t)$ and $J_0(t)$ defined in (19). Taking $K_1, K_2 \in \mathbb{R}^{1 \times N}$ such that $[K_1 \ K_2] = (\rho_u + \rho_\infty)^{-1} B^\top P$, we have that

$$u = - \begin{bmatrix} K_1 & 0 & K_2 & 0 \end{bmatrix} z^{N+1}$$

guarantees $\bar{J}_0(t) = J_0(t) + J_{N+1}(t) \leq 0$. Note that $\bar{J}_0(t)$ is $J_0(t)$ with N replaced by $N + 1$. By [33, Theorem 6.3.6], (3) has a solution for the matrices defined in (18) and (23) with N replaced by $N + 1$. That is, the same γ is achievable with $N + 1$ modes. When considering $N + 1$ modes, we are making the sum $J_0(t) + J_{N+1}(t)$ negative instead of each term, $J_0(t)$ and $J_{N+1}(t)$, independently. This gives more flexibility and may reduce γ , as demonstrated in Fig. 3.

4 Numerical simulations

As an example, we consider an aluminum rectangular beam of dimensions $1 \text{ m} \times 0.1 \text{ m} \times 0.01 \text{ m}$ with hinged ends and a piezoelectric actuator of length 2 cm placed at 30 cm from the left edge. This system can be modeled by (5) with the parameters given in the following table:

Linear density	μ	2.71 kg/m
Young’s modulus	E	$70 \times 10^9 \text{ N/m}^2$
Moment of inertia	I	$8.3 \times 10^{-8} \text{ m}^4$
Viscous damping	c_v	$1.76 \text{ kg}/(\text{m} \cdot \text{s})$
Structural damping	c_k	$2.05 \times 10^5 \text{ kg}/(\text{m} \cdot \text{s})$
Left actuator position	\tilde{x}_L	0.29 m
Right actuator position	\tilde{x}_R	0.31 m

The linear density is calculated as $\mu = \rho A$, where $\rho = 2710 \text{ kg/m}^3$ is the density of aluminum, and $A = 0.1 \times 0.01 = 10^{-3} \text{ m}^2$ is the cross-section area of the beam. The damping coefficients, c_v and c_k , are taken from [41]. The value of c_a depends on the type of the piezoelectric patch; it does not affect the performance analysis since the control can be scaled as $\tilde{u}' = c_a \tilde{u}$. After the change of variables (7), we obtain (8) with

$$c_1 = 1.4 \times 10^{-3}, \quad c_2 = 1.3 \times 10^{-3}, \quad x_L = 0.91, \quad x_R = 0.97.$$

Our objective is to design a state-feedback control law of the form (24) guaranteeing that the solution of (8) with $z(\cdot, 0) \equiv 0 \equiv z_t(\cdot, 0)$ satisfies (13) with $\rho_u = 10^{-3}$, $\rho_x = 0.1$, and smallest possible $\gamma > 0$. To decide on how many modes to consider in the controller design, we calculate the minimum γ for different numbers of controlled modes, N . Proposition 2 gives $\gamma_0 \approx 380$ as the smallest L^2 gain without control. For each integer $N \in [1, 40]$, we found the minimum γ satisfying the conditions of Theorem 1. The results are shown in Fig. 3. As explained in Remark 9, the L^2 gain decreases when more modes are considered. The limit value is $\gamma \approx 18$. Since γ does not improve significantly

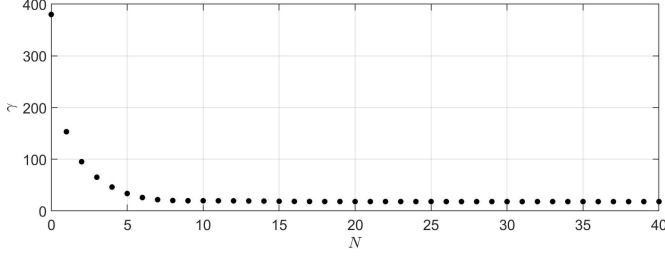


Fig. 3. The L^2 gain of the Euler–Bernoulli beam (8) for different numbers of controlled modes N .

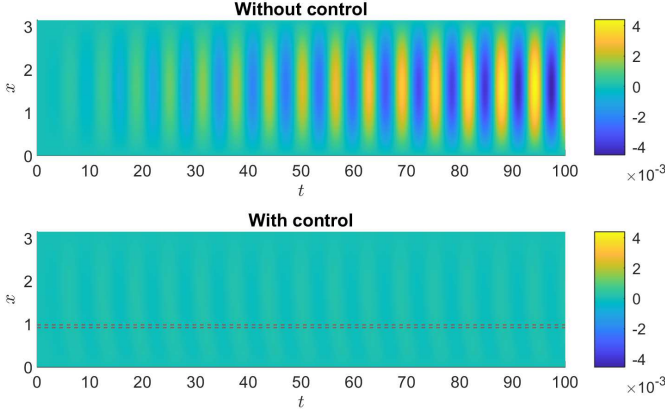


Fig. 4. Euler–Bernoulli beam without and with control. The red dashed lines show the ends of the piezoelectric actuator.

for $N > 8$, we consider $N = 8$ modes. In this case, $\gamma \approx 20.2$ and $\rho_\infty \approx 8 \times 10^{-3}$, which we found using (22). To find the controller gain in (24), we solve (3) for $P > 0$ with A , B , C , D , and E defined in (18) and (23). Note that, for this example, the first condition in (15) of [22] requires $N \geq 32$ and the resulting LMIs are not feasible for any $\gamma > 0$.

The results of numerical simulations without and with control for the same disturbance are shown in Fig. 4. The considered disturbance is the worst one for (17a) with $N = 30$ generated following the procedure in Remark 2. Namely, we calculated $P > 0$ satisfying (4) with A , E , and C given in (18) and (23), found $z_d^N(t)$ as the solution of (17a) with $N = 30$, $u \equiv 0$, and $z_d^N(0) = [1, \dots, 1]^T \in \mathbb{R}^{60}$, substituted $w^N(t) = \gamma^{-2} E^T P z_d^N(t)$ into (18), and took $w(x, t) = \sum_{n=1}^N w_n(t) \varphi_n(x)$. Clearly, the proposed control strategy attenuates the effect of the disturbance. This is also evident from Fig. 5, which shows

$$\|z(\cdot, t)\|_J = \sqrt{\|z(\cdot, t)\|^2 + \rho_x \|z_{xx}(\cdot, t)\|^2} \quad (27)$$

without (black) and with (blue) control.

The value of $J(t)$, obtained by replacing ∞ with t in (13), is shown in Fig. 6. As guaranteed by Theorem 1, the control ensures that $J = \lim_{t \rightarrow \infty} J(t) < 0$ for $\gamma \approx 20.2$ (blue line). Without control (black line), $J(t)$ becomes positive for $t \approx 70$. If the residue is ignored ($\rho_\infty = 0$), a smaller $\gamma \approx 7.16$ is obtained following the steps detailed in Section 3.2. In this case, the spillover phenomenon causes $J(t) > 0$ for $t > 7$

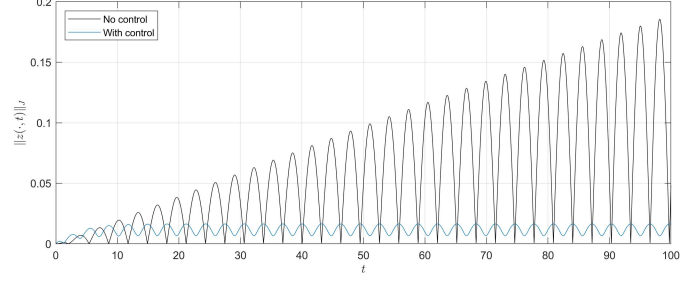


Fig. 5. The value of $\|z(\cdot, t)\|_J$, defined in (27), without (black) and with (blue) control.

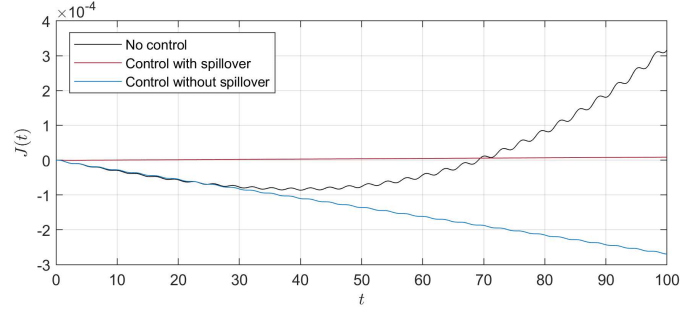


Fig. 6. The value of $J(t)$ (given by (13) with ∞ replaced by t) without control (black) and with control (blue) for $\gamma \approx 20.2$. The red line shows the spillover phenomenon occurring when the modes with $n > 8$ are ignored.

(red line). This vividly demonstrates why the residue, i.e., the modes with $n > N$, cannot be ignored. Theorem 1 provides a simple way of designing a controller avoiding the spillover phenomenon.

Remark 10 (N vs γ with spillover) *If the residue is ignored ($\rho_\infty = 0$), then $\gamma \approx 6.97$ for $N = 5$ (see Section 3.2) and $\gamma \approx 7.16$ for $N = 8$ (as explained above). That is, the L^2 gain may increase when more modes are considered. This happens because, by increasing N , one obtains a more accurate estimate of the actual L^2 gain, which is larger than that obtained using the truncated modal decomposition. If the residue is accounted for, larger N will never lead to a larger γ (see Remark 9).*

5 Conclusions

We studied the H_∞ control of the Euler–Bernoulli beam with viscous and Kelvin–Voigt damping using piezoelectric actuators. We showed that spillover occurs when a finite number of modes are considered in the H_∞ design. Then we proposed a simple modification of the cost guaranteeing that the controller designed based on a finite number of modes does not lead to spillover. Using a realistic model of the beam, we demonstrated how to find the number of modes required to design a controller, i.e., such that a further increase of the number of considered modes does not improve the L^2 gain significantly. Future work will be dedicated to designing output feedback, considering multiple

actuators and sensors, and treating the control input as a structured disturbance in the residue (Remark 6).

References

- [1] H. Özbay, “Tutorial review H_∞ optimal controller design for a class of distributed parameter systems,” *International Journal of Control*, vol. 58, no. 4, pp. 739–782, 1993.
- [2] B. van Keulen, *H_∞ -Control for Distributed Parameter Systems: A State-Space Approach*. Birkhäuser Boston, 1993.
- [3] M. Athans, “Toward a practical theory for distributed parameter systems,” *IEEE Transactions on Automatic Control*, vol. 15, no. 2, pp. 245–247, 1970.
- [4] M. J. Balas, “Toward A More Practical Control Theory for Distributed Parameter Systems,” in *Advances in Theory and Applications* (C. Leondes, ed.), vol. 18, pp. 361–421, Academic Press, 1982.
- [5] R. Triggiani, “Boundary Feedback Stabilizability of Parabolic Equations,” *Applied Mathematics and Optimization*, vol. 6, no. 1, pp. 201–220, 1980.
- [6] M. J. Balas, “Trends in Large Space Structure Control Theory: Fondest Hopes, Wildest Dreams,” *IEEE Transactions on Automatic Control*, vol. 27, no. 3, pp. 522–535, 1982.
- [7] R. F. Curtain, *A Comparison of finite-dimensional controller designs for distributed parameter systems*. [Research Report] RR-1647, INRIA. 1992.
- [8] P. D. Christofides, *Nonlinear and Robust Control of PDE Systems*. Birkhäuser Boston, 2001.
- [9] M. J. Balas, “Feedback Control of Flexible Systems,” *IEEE Transactions on Automatic Control*, vol. 23, no. 4, pp. 673–679, 1978.
- [10] L. Meirovitch and H. Baruh, “On the problem of observation spillover in self-adjoint distributed-parameter systems,” *Journal of Optimization Theory and Applications*, vol. 39, no. 2, pp. 269–291, 1983.
- [11] J. Bontsema and R. F. Curtain, “A Note on Spillover and Robustness for Flexible Systems,” *IEEE Transactions on Automatic Control*, vol. 33, no. 6, pp. 567–569, 1988.
- [12] M. J. Balas, “Finite-dimensional controllers for linear distributed parameter systems: Exponential stability using residual mode filters,” *Journal of Mathematical Analysis and Applications*, vol. 133, no. 2, pp. 283–296, 1988.
- [13] S. O. R. Moheimani, “Minimizing the Effect of Out of Bandwidth Modes in Truncated Structure Models,” *Journal of Dynamic Systems, Measurement, and Control*, vol. 122, no. 1, pp. 237–239, 1998.
- [14] C. Harkort and J. Deutscher, “Finite-dimensional observer-based control of linear distributed parameter systems using cascaded output observers,” *International Journal of Control*, vol. 84, no. 1, pp. 107–122, 2011.
- [15] I. Karafyllis and M. Krstic, “ISS With Respect To Boundary Disturbances for 1-D Parabolic PDEs,” *IEEE Transactions on Automatic Control*, vol. 61, no. 12, pp. 1–23, 2016.
- [16] I. Karafyllis, “Lyapunov-based boundary feedback design for parabolic PDEs,” *International Journal of Control*, vol. 94, no. 5, pp. 1247–1260, 2021.
- [17] R. Katz and E. Fridman, “Constructive method for finite-dimensional observer-based control of 1-D parabolic PDEs,” *Automatica*, vol. 122, p. 109285, 2020.
- [18] R. Katz and E. Fridman, “Delayed finite-dimensional observer-based control of 1D parabolic PDEs via reduced-order LMI,” *Automatica*, vol. 142, 2022.
- [19] H. Lhachemi and C. Prieur, “Predictor-based output feedback stabilization of an input delayed parabolic PDE with boundary measurement,” *Automatica*, vol. 137, p. 110115, 2022.
- [20] R. Katz and E. Fridman, “Global stabilization of a 1D semilinear heat equation via modal decomposition and direct Lyapunov approach,” *Automatica*, vol. 149, p. 110809, 2023.
- [21] R. Katz and E. Fridman, “Finite-Dimensional Boundary Control of the Linear Kuramoto-Sivashinsky Equation Under Point Measurement With Guaranteed L^2 -Gain,” *IEEE Transactions on Automatic Control*, vol. 67, no. 10, pp. 5570–5577, 2022.
- [22] A. Selivanov and E. Fridman, “Disturbance attenuation in the Euler–Bernoulli beam with viscous and Kelvin–Voigt damping via piezoelectric actuators,” in *IEEE Conference on Decision and Control*, 2023.
- [23] E. F. Crawley and J. De Luis, “Use of piezoelectric actuators as elements of intelligent structures,” *AIAA Journal*, vol. 25, no. 10, pp. 1373–1385, 1987.
- [24] E. K. Dimitriadis, C. R. Fuller, and C. A. Rogers, “Piezoelectric Actuators for Distributed Vibration Excitation of Thin Plates,” *Journal of Vibration and Acoustics*, vol. 113, no. 1, pp. 100–107, 1991.
- [25] K. Lenz, H. Özbay, A. Tannenbaum, J. Turi, and B. Morton, “Frequency domain analysis and robust control design for an ideal flexible beam,” *Automatica*, vol. 27, no. 6, pp. 947–961, 1991.
- [26] D. Halim and S. O. Moheimani, “Spatial resonant control of flexible structures — application to a piezoelectric laminate beam,” *IEEE Transactions on Control Systems Technology*, vol. 9, no. 1, pp. 37–53, 2001.
- [27] M. Tucsnak, “Regularity and Exact Controllability for a Beam with Piezoelectric Actuator,” *SIAM Journal on Control and Optimization*, vol. 34, no. 3, pp. 922–930, 1996.
- [28] E. Crépeau and C. Prieur, “Control of a clamped-free beam by a piezoelectric actuator,” *ESAIM – Control, Optimisation and Calculus of Variations*, vol. 12, no. 3, pp. 545–563, 2006.
- [29] H. Lhachemi and R. Shorten, “Boundary input-to-state stabilization of a damped Euler-Bernoulli beam in the presence of a state-delay,” *arXiv:1912.01117*, 2019.
- [30] Y. Cheng, Y. Li, Y. Wu, and K.-S. Hong, “Anti-disturbance control for a nonlinear flexible beam with velocity disturbance at the boundary,” *Automatica*, vol. 152, p. 110978, 2023.
- [31] D. Halim and S. Moheimani, “Experimental implementation of spatial H-infinity control on a piezoelectric-laminate beam,” *IEEE/ASME Transactions on Mechatronics*, vol. 7, no. 3, pp. 346–356, 2002.
- [32] A. Belyaev, A. Fedotov, H. Irschik, M. Nader, V. Polyanskiy, and N. Smirnova, “Experimental study of local and modal approaches to active vibration control of elastic systems,” *Structural Control and Health Monitoring*, vol. 25, no. 2, 2018.
- [33] M. Green and D. Limebeer, *Linear Robust Control*. Dover Publications, 2012.
- [34] D. L. Russell, “On Mathematical Models for the Elastic Beam with Frequency-Proportional Damping,” in *Control and Estimation in Distributed Parameter Systems*, pp. 125–169, Society for Industrial and Applied Mathematics, 1992.
- [35] L. Herrmann, “Vibration of the Euler-Bernoulli Beam with Allowance for Dampings,” in *World Congress on Engineering*, pp. 901–904, 2008.
- [36] G. Chen and D. L. Russell, “A mathematical model for linear elastic systems with structural damping,” *Quarterly of Applied Mathematics*, vol. 39, no. 4, pp. 433–454, 1982.
- [37] A. Pazy, *Semigroups of Linear Operators and Applications to Partial Differential Equations*, vol. 44. Springer New York, 1983.

- [38] M. Tucsnak and G. Weiss, *Observation and Control for Operator Semigroups*. Birkhäuser Basel, 2009.
- [39] S. Timoshenko, *Strength of Materials. Part 1*. Van Nostrand, 1955.
- [40] G. Hardy, J. Littlewood, and G. Pólya, *Inequalities*. Cambridge University Press, 1952.
- [41] H. T. Banks and D. J. Inman, “On Damping Mechanisms in Beams,” *Journal of Applied Mechanics*, vol. 58, no. 3, pp. 716–723, 1991.

A Solution of (20)

Let $P_n = \begin{bmatrix} p_1 & p_2 \\ p_2 & p_3 \end{bmatrix}$. Then (20) is equivalent to

$$\begin{aligned} \alpha_n p_2^2 - 2\omega_n^2 p_2 + (1 + \rho_x \omega_n^2) &= 0, \\ p_1 - 2\zeta_n \omega_n p_2 - p_3 \omega_n^2 + \alpha_n p_2 p_3 &= 0, \\ \alpha_n p_3^2 - 4\zeta_n \omega_n p_3 + 2p_2 &= 0 \end{aligned}$$

with $\alpha_n = b_n^2/\rho_n + \gamma^{-2}$. These are equivalent to

$$\begin{aligned} p_2 &= \alpha_n^{-1} \left[\omega_n^2 \pm \sqrt{\omega_n^4 - \alpha_n(1 + \rho_x \omega_n^2)} \right], \\ p_3 &= \alpha_n^{-1} \left[2\zeta_n \omega_n \pm \sqrt{4\zeta_n^2 \omega_n^2 - 2\alpha_n p_2} \right], \\ p_1 &= 2\zeta_n \omega_n p_2 + p_3 \omega_n^2 - \alpha_n p_2 p_3. \end{aligned} \quad (\text{A.1})$$

These values are real if and only if

$$\omega_n^4 \geq \alpha_n(1 + \rho_x \omega_n^2) \quad \text{and} \quad (\text{A.2a})$$

$$2\zeta_n^2 \omega_n^2 \geq \alpha_n p_2 = \omega_n^2 - \sqrt{\omega_n^4 - \alpha_n(1 + \rho_x \omega_n^2)}. \quad (\text{A.2b})$$

We took p_2 with “ $-$ ” since $2\zeta_n^2$ can be smaller than 1.

To minimize ρ_n , we maximize α_n . If $2\zeta_n^2 \geq 1$, then (A.2b) is true subject to (A.2a), which gives $\alpha_n = \omega_n^4/(1 + \rho_x \omega_n^2)$. Substituting this into (A.1), we obtain

$$P_n = \frac{\omega_n}{\alpha_n} \begin{bmatrix} 2\zeta_n \omega_n^2 & \omega_n \\ \omega_n & 2\zeta_n \pm \sqrt{4\zeta_n^2 - 2} \end{bmatrix} > 0.$$

If $2\zeta_n^2 < 1$, then (A.2b) gives the maximum $\alpha_n = 4\omega_n^4 \zeta_n^2 (1 - \zeta_n^2)/(1 + \rho_x \omega_n^2)$, which satisfies (A.2a) since $\omega_n^4 - \alpha_n(1 + \rho_x \omega_n^2) = \omega_n^4 (1 - 2\zeta_n^2)^2 > 0$. Substituting this into (A.1), we obtain

$$P_n = \frac{2\zeta_n \omega_n}{\alpha_n} \begin{bmatrix} \omega_n^2 & \zeta_n \omega_n \\ \zeta_n \omega_n & 1 \end{bmatrix} > 0.$$

The minimum values of ρ_n are calculated from $\alpha_n = b_n^2/\rho_n + \gamma^{-2}$ with the corresponding α_n .

B Upper bound on the L^2 gain for the residue

For $n > M$, we have $\zeta_n \geq 1/\sqrt{2}$. Then

$$\begin{aligned} \rho_n &= \frac{b_n^2(1 + \rho_x \omega_n^2)}{\omega_n^4 - (1 + \rho_x \omega_n^2)\gamma^{-2}} = \frac{\omega_n^{-2} + \rho_x}{1 - (\omega_n^{-2} + \rho_x)\omega_n^{-2}\gamma^{-2}} \frac{b_n^2}{\omega_n^2} \\ &\leq \frac{\omega_{M+1}^{-2} + \rho_x}{1 - (\omega_{M+1}^{-2} + \rho_x)\omega_{M+1}^{-2}\gamma^{-2}} \frac{b_n^2}{\omega_n^2} = C_M \frac{b_n^2}{\omega_n^2}. \end{aligned}$$

Note that b_n/ω_n are the Fourier coefficients of

$$\chi_{[x_L, x_R]}(x) = \begin{cases} 1, & x \in [x_L, x_R], \\ 0, & x \notin [x_L, x_R]. \end{cases}$$

By Parseval’s identity,

$$\sum_{n=1}^{\infty} \frac{b_n^2}{\omega_n^2} = \|\chi_{[x_L, x_R]}\|^2 = |x_R - x_L|.$$

Therefore,

$$\sum_{n=M+1}^{\infty} \rho_n \leq C_M \sum_{n=M+1}^{\infty} \frac{b_n^2}{\omega_n^2} = C_M \left[|x_R - x_L| - \sum_{n=1}^M \frac{b_n^2}{\omega_n^2} \right],$$

which implies (22).